Redistribution of Implanted Noble Gas Atoms by Self-Interstitials in Molybdenym and Nickel

Veen, A. van; Buters, W.Th.M.; Armstrong, T.R.; Nielsen, B.; Westerduin, K.T.; Caspers, L.M.; Hosson, J.Th.M. De

Published in:
Nuclear Instruments And Methods In Physics Research

DOI:
10.1016/0167-5087(83)90920-1

Publication date:
1983

Nuclear Instruments and Methods 209/210 (1983) 1055–1061
North-Holland Publishing Company

REDISTRIBUTION OF IMPLANTED NOBLE GAS ATOMS BY SELF-INTERSTITIALS IN MOLYBDENUM AND NICKEL

A. VAN VEEN, W.Th.M. BUTERS, T.R. ARMSTRONG, B. NIELSEN, K.T. WESTERDUIN and L.M. CASPERS

University of Technology Delft, Interuniversity Reactor Institute, Mekelweg 15, 2629 JB Delft, The Netherlands

J.Th.M. DE HOSSON

Department of Applied Physics, Materials Science Center, University of Groningen, Nijenborgh 18, 9747 AG, The Netherlands

Thermal Desorption Spectrometry (TDS) has been used to study the interactions of Self-Interstitial Atoms (SIA) with noble gas associated defects in Mo and Ni. Low energy heavy ion bombardment (100 eV Ar and Xe for Mo; 50 eV Kr for Ni) has been used to introduce SIA into the metals. Interactions have been observed of SIA with He_nV (V = Vacancy; $n = 1, \ldots, 7$) and ArV_n ($n = 1, 2, \cdots$) in Mo, and with NeV in Ni. In all these cases the defects were found to be reduced by SIA capture. Substitutional atoms were converted into (at 300 K) mobile interstitials. For Kr in Ni no capture of SIA was observed. The results and their possible consequences for noble gas agglomeration in noble gas irradiated metals are discussed.

1. Introduction

The agglomeration of noble gas atoms implanted in metals is a well known phenomenon observed by transmission electron microscopy. Typical conditions for the phenomenon to occur are fluences of $\sim 10^{15}$ at cm^{-2} at energies > 1 keV. An intriguing fact is that the gas agglomerates are formed also at temperatures where transport of the implanted atoms via vacancy assisted diffusion - possibly "radiation enhanced" by vacancies produced during the bombardment - can be neglected. Sass and Eyre observed this effect for different noble gases in Mo [1]. Mazey et al. observed this effect for room temperature bombardment of Mo with He [2]. Johnson and Mazey observed similar behaviour of He in Ni [3]. De Hosson reported on clustering of Ar in Cu [4] irradiated at room temperature.

With regard to helium it was known already [5] that in the absence of traps helium is interstitially mobile at room temperature in metals. This behaviour of helium may explain clustering. But the question remains what role the part of the helium captured by small vacancy complexes may play in the further evolution of the clustering process. For the other noble gas projectiles it is assumed that they come to rest as substitutional atoms and therefore can move only when assisted by mobile vacancies. However, recent experiments [6] have shown that reactions with self-interstitials occur which lead to the formation of room temperature mobile noble gas interstitials.

In this paper it is proposed that the conversion of substitutional atoms into interstitials by interaction of Self-Interstitial Atoms (SIA) is an important mechanism for redistribution during ion implantation. Results are reported on the interaction of SIA with noble gas associated defects. Characterization of the defects before and after the SIA interaction is performed by Thermal Desorption Spectrometry (TDS). Since the TDS technique is useful for monitoring defect populations only when moderate defect concentrations are present at shallow depth below the surface (< 100 nm) the experimental work is concerned with low fluences (10^{12} at. cm^{-2}) of keV ions. The experimental results are used in a rate theory model (Monte Carlo calculations) in order to give estimates of redistribution processes occuring at higher fluences.

2. Experimental

2.1. The TDS measuring technique

In earlier articles by the authors [7,8] and by Kornelsen and Van Gorkum [5,9] the technique

0167-5087/83/0000–0000/$03.00

Table 1
Desorption peak assignments [a]

Peak assignment	T (100 K)	Release reaction
Mo(110)		
H	11.8	$HeV \rightarrow V + He$
G	9	$He_2V \rightarrow HeV + He$
F	8.5	$He_3V \rightarrow He_2V + He$
H′	11.5	$HeArV_2 \rightarrow ArV_2 + He$
G′	9.8	$He_2ArV_2 \rightarrow HeArV_2 + He$
A	6.0	$HeArV \rightarrow ArV + He$
B	7.6	$He_2ArV \rightarrow HeArV + He$
Ni(110)	11	neon diffusion
	< 9	surface related
	10	krypton diffusion
	8	surface related

[a] See also ref. 6 for Mo and ref. 13 for Ni.

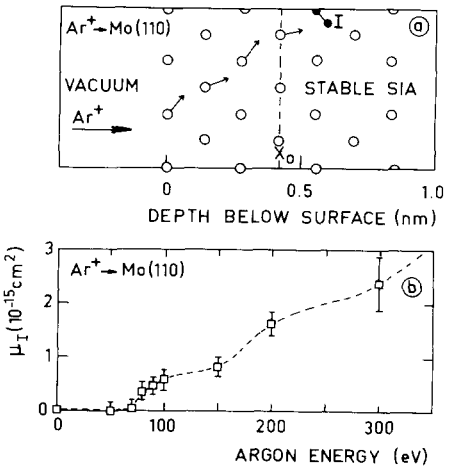

Fig. 1. (a) Schematic drawing of SIA formation below the surface of a bcc (110) crystal via a replacement sequence in the ⟨111⟩ direction. (b) The SIA capture rate coefficient versus kinetic energy, measured for 3×10^{11} cm^{-2} (deep) HeV defects in Mo(110).

and aspects of the analysis of the desorption spectra are described. Briefly, the release of trapped gas during ramp heating (~ 40 K/s) of the irradiated sample is monitored by a quadrupole mass spectrometer. The sample preparation may consist of subsequent irradiation and annealing procedures in order to create well defined defect populations, e.g. exclusively substitutional noble gas atoms denoted by XV with X = He, Ne, Ar etc. and V = Vacancy.

In the final stage of preparation low energy helium may be injected which causes no further damage but is used to decorate the defects with trapped helium. The desorption spectrum of the helium or the other implanted gases is generally a composition of release peaks at different temperatures varying in shape due to the different types of release mechanisms, e.g., first order, diffusion or complex release mechanisms when traps are multiply occupied by gas atoms. Until now helium desorption peaks due to He$_n V$ and He$_n XV$ dissociation (n = number of helium atoms) have been assigned. Desorption peaks of the other noble gases are assigned to vacancy assisted diffusion of the gas and release from surface associated trapping sites. In table 1 the peak assignments are given of the desorption peaks which will be considered in this article.

2.2. The method for introduction of self-interstitials

Self-interstitials (SIA) are introduced into the metal by low energy heavy ion bombardment of the metal surface. Fig. 1a shows schematically the formation of SIA at some depth below the surface via a replacement collision sequence (r.c.s.) induced by an Ar ion impact at the surface. The SIA at depths smaller than a certain depth x_0, called the recombination depth, will recombine spontaneously with the surface in a process analogous to recombination of Frenkel pairs [10]. Those SIA formed beyond x_0, if mobile, will start a random walk and can in principle visit lattice sites of an undamaged crystal up to large depths. In cases when defects able to capture the SIA are present it can be derived [8] that the SIA capture rate coefficient μ_I, defined by $\mu_I = -1/N\, dN/dP$ (N = the areal density of the traps, and P the irradiation dose of noble gas ions) is well approximated by

$$\mu_I = 4\alpha_I z_I a_0(\langle x\rangle - x_0) \qquad (1)$$

for defects deeper than $\langle x\rangle$, where:

α_I = the yield (SIA per ion) of SIA at depth $> x_0$;
z_I = a trapping constant dpendent on the defect type ($z = 5$ for SIA-trapping in a monovacancy [11];
a_0 = the lattice constant;
$\langle x\rangle$ = the averaged depth of SIA at depths $x > x_0$;
x_0 = recombination depth.

For defects in the interval from $x = x_0$ to $x = \langle x\rangle$

μ_1 rises linearly from $\mu_1 = 0$ to the value in (1).

Fig. 1b. shows the measured influence of the kinetic energy of Ar ions on the rate coefficient μ_1 measured for HeV defects in Mo(110). The threshold energy for the SIA production is found to be around ~ 80 eV. Similar experiments for Ni(110) give a threshold of ~ 30 eV. A discussion of these numbers and further details on the methods will be published elsewhere [12].

3. Experimental results on interactions of SIA with defects.

3.1. Helium in molybdenum

A Mo crystal containing only HeV defects can be prepared by a low dose 3 keV He ion irradiation and subsequent ramp annealing to 1040 K (40 K/s). Figs. 2a and b show these different stages of the defect preparation. In fig. 2a the helium spectrum is plotted for an irradiated crystal without annealing; desorption peaks assigned to HeV, He_2V, He_3V etc. are seen (F, G, H peaks; see also table 1). Furthermore, empty vacancies are present in the crystal but these can be made visible only by further filling with low energy helium (not shown here). In fig. 2b the effect of the annealing is shown; the excess helium ($n > 1$) in the vacancies has gone and also empty vacancies have moved out of the crystal (checked by additional filling with helium). The result of the interaction of HeV with SIA before and after irradiation with 100 eV Xe is shown in fig. 2c. Apparently the amount of HeV has been reduced and the interstitial He produced in the reaction

$$\mathrm{He}V + I \rightarrow \mathrm{He\ (mobile)},$$

where I means interstitial, is for the major part (85%) released via the crystal surface and for the rest (15%) redistributed via the capture reactions

$$\mathrm{He} + \mathrm{He}V \rightarrow \mathrm{He}_2V \quad \text{and} \quad \mathrm{He} + \mathrm{He}_2V \rightarrow \mathrm{He}_3V,$$

which is observed by the appearance of G and F peaks in the spectrum. Helium filling experiments on the reduced HeV population prove that the HeV defects are completely removed by SIA interaction, i.e., not only the helium is released but also the SIA has recombined with the vacancy [8]. Analogous experiments but then for multiply filled vacancies (not shown here) give as result that SIA recombination with He_nV is prohibited for a filling larger than 7 helium:

$$\mathrm{He}_nV + I \rightarrow n\mathrm{He} \quad \text{for } n \leqslant 7 \text{ only}.$$

The results of variation of the 100 eV Xe dose are shown in fig. 4a. It is observed that the slope of the curve (initially corresponding with $\mu_1 = 7 \times 10^{-16}$ cm^2) becomes less for high Xe dose ($p > 1 \times 10^{15}$ at. cm^{-2}).

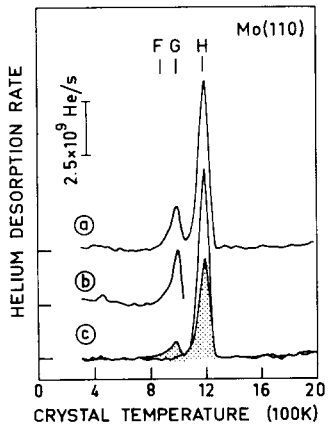

Fig. 2. Helium desorption spectra for (a) defects created by 2×10^{12} cm^{-2} 3 keV He, (b) partial annealing ($T_a = 1040$ K) of these defects (c) before and after (shaded spectrum) irradiation with 100 eV Xe (5×10^{14} cm^{-2}). See table 1 for explanation of desorption peak assignments.

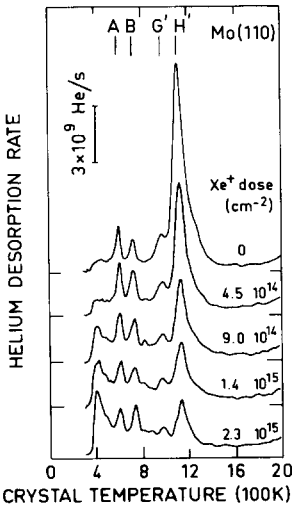

Fig. 3. Helium desorption spectra showing the effect of SIA capture on a mixed ArV and Ar_nV ($n > 1$) population for various doses of 100 eV Xe. The Ar defects were prepared by 2×10^{12} cm^{-2} 2 keV Ar irradiation and subsequently annealed to 800 K. The defects were decorated by 150 eV He irradiation (10^{13} cm^{-2}). See table 1 for explanation of desorption peak assignments.

3.2. Argon in molybdenum

It was shown by us that ArV defects (substitutional argon) can be prepared in Mo by annealing a 2 keV Ar irradiated crystal to a temperature > 1000 K [6]. Annealing at a lower temperature (T_a = 800 K) gives a mixed population of ArV and ArV_2, ArV_3 defects. Since vacancies become mobile at $T_a \approx 500$ K, in both cases no single vacancies are present in the crystal. In fig. 3 the top spectrum shows the helium desorption peaks due to helium release from helium decorated ArV (A and B peak) and ArV_n(G′ and H′ peak) for the 800 K annealed crystal. The other curves show the evolution of the spectrum when the crystal is bombarded with increasing doses of 100 eV Xe ions.

In fig. 4b the defect population of ArV (1200 K annealing) is plotted versus the 100 eV Xe dose. A rapid decrease of the ArV populaton is observed ($\mu \approx 1 \times 10^{-15}$ cm^2) for Xe doses $p < 10^{15}$ at cm^{-2}. Beyond a Xe dose $p = 1 \times 10^{15}$ at cm^{-2} the slope of the curve becomes less, similar to what was observed for HeV (fig. 4a).

In fig. 4c the ArV and ArV_n populations, derived from the helium peak populations of fig. 3, are plotted versus the Xe dose. Now it is observed that the ArV population initially remains constant while the ArV_n population rapidly decreases with dose. Apparently the removal of ArV is balanced by the production of new ArV via the interstitial capture reaction

$$\mathrm{Ar}V_2 + I \rightarrow \mathrm{Ar}V \qquad \text{and} \qquad \mathrm{Ar}V_3 + 2I \rightarrow \mathrm{Ar}V,$$

so that the ArV population decreases only if the ArV_n population is sufficiently reduced. Earlier we reported the results of experiments in which the SIA–Ar interaction was monitored by argon desorption [6]. In agreement with the present results much less Ar release from the crystal was observed in the case of 800 K annealing than in the case of 1200 K annealing; the stepwise reduction of ArV_n complexes (800 K) required capture of more SIA.

The Ar interstitials formed in these experiments (low defect concentrations) are found partly to be released from the crystal and partly to be retrapped in surface related states. One can envisage that at higher concentrations a substantial fraction of the Ar is retrapped at the other defects. As a consequence the Ar is redistributed and Ar clusters will be formed under room temperature condition.

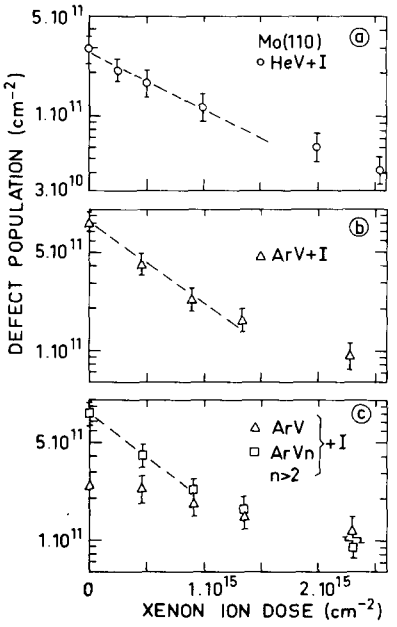

Fig. 4. Defect population versus 100 eV Xe dose for (a) HeV defects (see also fig. 2), (b) substitutional Ar (ArV), and (c) a mixed population of ArV and ArV_n($n > 1$) defects. Defect populations have been derived from helium desorption spectra.

3.3. Helium, neon and krypton in nickel

Data on low dose noble gas implantation in Ni (fcc) are rather scarce. In particular, peak assignments of helium desorption from He-decorated noble gas atoms are not yet thoroughly investi-

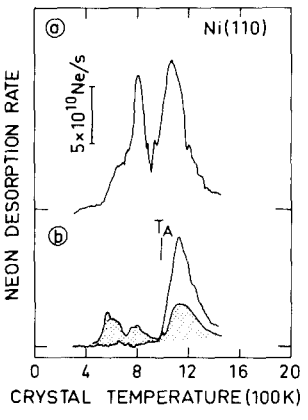

Fig. 5. Neon desorption spectra dor (a) neon associated defects created by 3 keV Ne irradiation (1.4×10^{12} cm^{-2}), and (b) the same defects annealed to T_a = 1000 K, before and after (shaded spectrum) irradiation with 50 eV Kr (5×10^{14} cm^{-2}).

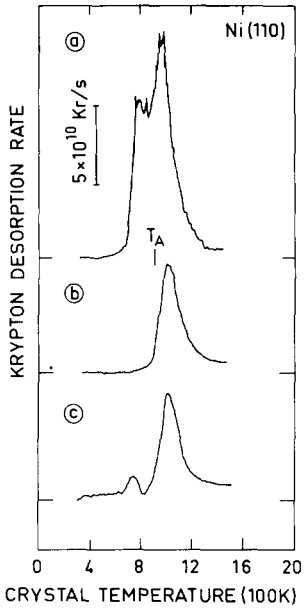

Fig. 6. Krypton desorption spectra showing the same stages of the SIA interaction experiment of fig. 5 but now for krypton. Irradiation doses are identical but $T_a = 900$ K. In (c) the result of SIA interaction is shown.

gated. Most of the available data have been reported by Kornelsen and Edwards [13,14]. nevertheless it seems of interest to present some preliminary results obtained for nickel. Substitutional atoms are prepared in Ni(110) by annealing after ion irradiation similar as described for Mo. However the required annealing temperatures are lower than for Mo: $T_a = 800$ K for HeV, $T_a = 1000$ K for NeV and $T_a = 900$ K for KrV. Low energy Kr (50 eV) is used to introduce SIA into the nickel crystal.

Helium: Similarly to what was observed for HeV in Mo we found reduction of the HeV population in Ni by SIA interaction (not further shown here).

Neon: Fig. 5a shows the neon desorption spectrum of the Ni crystal implanted with 3 keV Ne ions. Fig. 5b shows the desorption spectrum of the annealed (1000 K) crystal before and after the introduction of SIA. A fraction of 60% of the neon originally desorbed in the neon peak ascribed to vacancy assisted diffusion [13] has disappeared. Some of it is observed to be released at lower temperatures in peaks which are related with surface sites [13]. The remaining part apparently left the crystal. The result of this experiment is very much similar to what was found for ArV in Mo [6]. Therefore we may conclude that also NeV by interaction of SIA is converted into mobile Ne interstitials.

Krypton: fig. 6 shows the different stages of the SIA interaction experiment similar to those shown for Ne in fig. 5. It appears that the amount of krypton originally desorbed in the Kr diffusion peak is only slightly reduced. The explanation might be that KrV is stable against SIA capture or that KrV_n ($n > 1$) at $T_a = 900$ K has not been reduced to KrV.

4. Discussion

4.1. Surface effects

The description of SIA introduction and SIA interaction given in section 2.2 corresponds well to the observed phenomena when comparatively low doses of the ions used for SIA production are considered. However, in all cases we found a decrease of the SIA capture rate coefficient for increasing dose. A possible explanation for this effect might be the build up of surface damage which is not annealed at room temperature. Displaced atoms in the surface layers will disturb the collision processes which lead to distant SIA formation. There is no reason to assume that the implanted heavy ions play a decisive role. At 100 eV implantation energy it is measured that the maximum amount of Ar retained in surface-related trapping sites is $\sim 5 \times 10^{12}$ at. cm^{-2} corresponding to 0.005 fraction of the surface area. Therefore it is not likely that Ar causes this effect. Evans [15] investigated with TEM a Mo(100) crystal bombarded by us with a high dose of 100 eV Ar ions ($\sim 1 \times 10^{16}$ at. cm^{-2}) and found signs of surface damage. Another sign of surface damage is the increased trapping of low energy helium in surface-related sites when the crystal has been irradiated with high dose heavy ions, see e.g. the helium desorption in the temperature range 400–500 K in fig. 3.

Inherent to the use of low energy heavy ions the displacement rate of the atoms in the first layers will be high. Therefore the defects situated here will be subjected to a a dynamical release process rather than the thermal process of SIA interaction (μ_I) considered in this article. Removal rate coeffi-

cients measured by us for gas in surface related positions (He, Ar) are a factor 10–20 higher than μ_I. Fortunately, noble gases implanted in the first layers are released at temperatures lower than the T_a used here.

Furthermore, helium desorption peaks due to surface related noble gas defects can be distinguished from peaks due to deeper defects [16]. Release by sputtering processes can be excluded since the sputtering yield of 100 eV ions is of the order of 0.05 at/ion.

4.2. Energetics of the SIA interaction

Atomistic calculations on Ar in Mo [6] predict, in line with the experiment, the recombination of SIA with ArV under an energy release of 1.97 eV. The migration energy of the formed Ar interstitial is 0.33 eV (similar as for He). Melius et al [17] performed atomistic calculations on the noble gases in Ni. They predict NeV to be converted into a very mobile Ne interstitial (migration energy < 0.5 eV) under release of 1.41 eV energy. In contrast to Ne they predict for Kr the formation of a bound self interstitial. To break up the formed KrVI complex a dissociation energy of 1.04 eV is required. The binding of vacancies to KrV_2 is rather strong. A dissociation energy of 2.72 eV is quoted which corresponds to high dissociation temperatures ($\sim$ 1000 K). Both of these results could explain the experimental result found for Kr (section 3.3). Experimentally the configuration of Kr after high temperature annealing should be further established.

4.3. Redistribution of noble gases during keV ion irradiation

A Monte Carlo model is used to describe the evolution of the defect populations during noble gas ion bombardment. The model is similar to that described by Baskes et al [18] but includes the depth dependency of the defects. In table 2 defect populations are given for three different irradiation doses of 3 keV He on Mo(110). The average depths of implanted atoms and damage were 30 nm and 22 nm, respectively. Values for trapping constants are taken from [11], data on helium ranges are calculated with MARLOWE (see ref. 10), vacancy production data are quoted in [10]. The second irradiation dose corresponds with the dose used in fig. 2 (top spectrum). Although helium trapping appears to be underestimated, the agreement with the experimentally derived defect populations is reasonable. At the higher dose in table 2 it is seen that the probability for trapping of injected helium and retrapping of helium by SIA interactions has been strongly increased. A further increase of dose can lead to to nearly 100% removal of small helium vacancy complexes as has been demonstrated by Baskes et al with the earlier mentioned model calculations [18].

An important parameter in the model is the fraction of implanted noble gas atoms being in interstitial configuration after the spontaneous and correlated recombination processes in the cascade volume have been completed. For Ar one may argue that similar recombination takes place for the Frenkel pairs and for Ar (interstitial)–vacancy pairs where Ar might be formed by the Ar$V + I \rightarrow$ Ar reaction. An estimation is that 20% of the implanted Ar is free to move as an interstitial and will be available for redistribution (the surviving fraction of self-interstitials is $\sim$ 30% [10]). Table 3 shows defect populations obtained for 2 keV Ar irradiation of Mo obtained with the above mentioned model. Average depths of implanted atoms and damage were 1.8 nm and 1.1 nm, respectively.

Table 2
Defect population as a function of dose for 3 keV He in Mo(110).

Dose (10^{11} at cm^{-2})	Defect peak population (10^{11} at cm^{-2})			
	V	HeV	He$_2V$	He$_3V$
4	2	0.18	-	-
20	6.5	1.6 (2.9) [a]	0.26	0.11
100	15	8	3.5	1.9

[a] Values in parentheses are derived from experiments (fig. 2).

Table 3
Defect populations as a function of dose for 2 keV Ar in Mo(110).

Dose (10^{11} at cm^{-2})	Defect peak population (10^{11} at cm^{-2})		
	ArV_n $n > 1$	ArV	$\sum_{m,n} m\mathrm{Ar}_m V_n$, $m > 1$
4	2.1	0.36	-
20	9.9 (8) [a]	2.2 (2.5) [a]	0.09
100	32	11	3.1

[a] Values in parentheses are derived form experiments (fig. 4).

It can be seen that for an irradiation dose of 10^{13} at cm^{-2} a fraction of 8% of the Ar is fond in small agglomerates of argon.

5. Conclusions

Evidence is found for the redistribution of implanted noble gases by interaction of SIA for He and Ar in molybdenum and for Ne in Nickel. For Kr in Ni no influence of the SIA interaction was observed. this case needs to be investigated further.

Agglomeration of implanted noble gas atoms caused by SIA interacion is expected to play a role for Ar fluences $> 1 \times 10^{13}$ at. cm^{-2} in the case of 2 keV Ar irradiation.

References

[1] S.L. Sass and B.L. Eyre, Phil. Mag. 27 (1973) 1447–1453.
[2] D.J. Mazey, B.L. Eyre, J.H. Evans, S.K. Erents and G.M. McCracken, J. Nucl. Mat. (1977) 145.
[3] P.B. Johnson and D.J. Mazey, Nature 281 (1979) 359–360.
[4] J.Th.M. de Hosson, Phys. Stat. Sol. (A) 40 (1977) 293–301.
[5] E.V. Kornelsen, Rad. Effects 13 (1972) 227.
[6] A. Van Veen, W.TH.M. Buters, G.J. van der Kolk, L.M. Caspers and T.R. Armstrong, Nucl. Instr. and Meth. 194 (1982) 485–489.
[7] A. van Veen, L.M. Caspers, E.V. Kornelsen, R. Fastenau, A.A. van Gorkum and A. Warnaar, Phys. Stat. Sol. (A) 40 (1977) 235.
[8] A. van Veen and L.M. Caspers, Harwell Symp. on Inert Gases in Metals and Ionic Solids, ed., S.F. Pugh, AERE report 9733 (September 1979) p. 517.
[9] A.A. van Gorkum, thesis, Delft (1981) ch. 1 and 2; A.A. van Gorkum and E.V. Kornelsen, Vacuum, in press.
[10] M. Hou, A. van Veen, L.M. Caspers and M.R. Ypma, these Proceedings, p. 19.
[11] R.H.J. Fastenau, A. van Veen, P. Penning and L.M. Caspers, Phys. Stat. Sol. (A) 47 (1978) 577.
[12] A. van Veen, B. Nielsen, T.R. Armstrong, W.Th.M. Buters and L.M. Caspers, to be published in Rad. Effects.
[13] D.E. Edwards, Jr., J. Appl. Phys. 46 (1975) 1437.
[14] E.V. Kornelsen and D.E. Edwards, Jr., Applications of Ion Beams to Metals, eds., S.T. Picreaux et al. (Plenum, New York, 1974) p. 251.
[15] J.H. Evans, Private communication.
[16] R.H.J. Fastenau, A. van Veen, L.M. Caspers and M.R. Ypma, Rad. Effects 61 (1982) 143–149.
[17] C.F. Melius, W.D. Wilson and C.L. Bisson, Harwell Symp. on Inert gases in Metals and Ionic Solids, ed., S.F. Pugh, AERE Report 9733 (September 1979) p. 14.
[18] M.I. Baskes, R.H.J. Fastenau, P. Penning, L.M. Caspers and A. van Veen, J. Nucl. Mat. 102 (1981) 235–245.